

99% Efficiency True-Bridgeless Totem-Pole PFC

Based on GaN HEMTs

Liang Zhou, member IEEE and YiFeng Wu, member IEEE
Transphorm, Inc. 75 Castilian Dr., Goleta, CA, 93117 USA
lzhou@transphormusa.com

Abstract: This paper presents a true bridgeless totem-pole Power-Factor-Correction (PFC) circuit using GaN HEMT. Enabled by a diode-free GaN power HEMT bridge with low reverse-recovery charge, very-high-efficiency single-phase AC-DC conversion is realized using a totem-pole topology without the limit of forward voltage drop from a fast diode. When implemented with a pair of sync-rec MOSFETs for line rectification, 99% efficiency is achieved at 230V ac input and 400 dc output in continuous-current mode.

Keywords: single phase PFC, totem-pole bridgeless PFC, GaN HEMT, AC-DC

I. INTRODUCTION

Power Factor Correction (PFC) circuits are widely adopted for AC-DC power conversion. Conventional PFC converters comprise a full-wave diode bridge rectifier and a boost circuit. In the power delivery path there are 2 diode voltage drops at the input bridge and one at the boost stage, which set a hard limit on system efficiency. Trying to eliminate the diode bridge in the input, a family of bridgeless PFC converters was examined, including: Dual Boost Bridgeless PFC, Two boost-circuit bridgeless PFC, Bi-directional Bridgeless PFC, and Totem-pole bridgeless PFC [1]. Through a detail analysis and comparison of four bridgeless converters, it is concluded that Totem-pole bridgeless PFC converter uses the least components and has the smallest conduction loss among all bridgeless PFC topologies [2]. Paper [3] studied totem-pole converter in ZVS DCM/CCM boundary mode, with peak efficiency around 98.2% at 230Vac input. Paper [4] proposed an interleaved totem-pole PFC with limited benefit. Soft-switching was used in both implementations due to the high reverse recovery charges of Silicon MOSFET. The low inductance value required for DCM/CCM boundary operation exacerbates the zero-crossing current spike problem.

To pursuit higher efficiency, soft-switching methods and interleaved control are used in PFC. In paper [5], a 3.5KW PFC converter with transition-mode switching and complicated control reaches 99.2% efficiency for 230Vac input at the cost of 14 MOSFETs, which is not a practically solution.

The advent of GaN HEMT power device opens a new chapter in power electronics. Diode-free GaN hard-switched bridges have been developed with low switching loss, low Q_{rr} and low capacitance [6][7][8]. This enables simple and efficient power conversion circuits. As an application sample in PFC converter, this paper presents hard-switching totem-pole bridgeless PFC in CCM, which employs the simplest topology, yet offers very-high performance.

II. TOTEM-POLE BRIDGELESS PFC BASED ON GAN HEMT

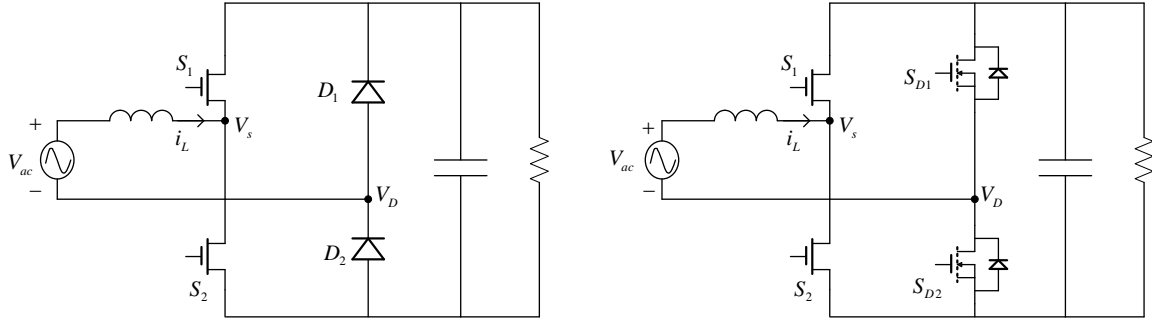


Fig.1 Totem-pole bridgeless PFC boost converter based on GaN HEMT (a) Diode for line rectification (b) MOSFET for line rectification

Fig.1 gives the totem-pole bridgeless topology. Fig.1(a) gives the implementation with two GaN HEMT and two slow diodes, while Fig.1(b) gives the implementation with two GaN HEMT and two Silicon MOSFETs, which are used to replace the diode to further boost the efficiency. The topology in Fig.1(b) looks the same as any single-phase converter, but it is controlled as the original totem-pole bridgeless PFC in Fig.1(a), hence it is labeled the totem-pole bridgeless PFC with MOSFET for line rectification.

The operation principle of totem-pole PFC is illustrated in Fig.2 for two half-cycle respectively. In the positive AC line half-cycle, D2 is conducting and connecting the AC source to the output ground. S2 is the active boost switch and S1 freewheels the inductor current and discharges inductor energy to power the output. S1 will also be turn-on complementary during the inductor current freewheeling to reduce the conduction loss. In the negative AC line half cycle, D1 is conducting and connecting the AC source to the output DC bus. S1 is the active boost switch and S2 freewheels the inductor current. The operation mode changes at each AC zero-crossing. In positive half, the PWM determined by boost duty ratio is driving switch S2, while it is driving switch S1 in the negative half. The operation of MOSFET version is the same except that the MOSFET is actively turned on for half cycle line rectification.

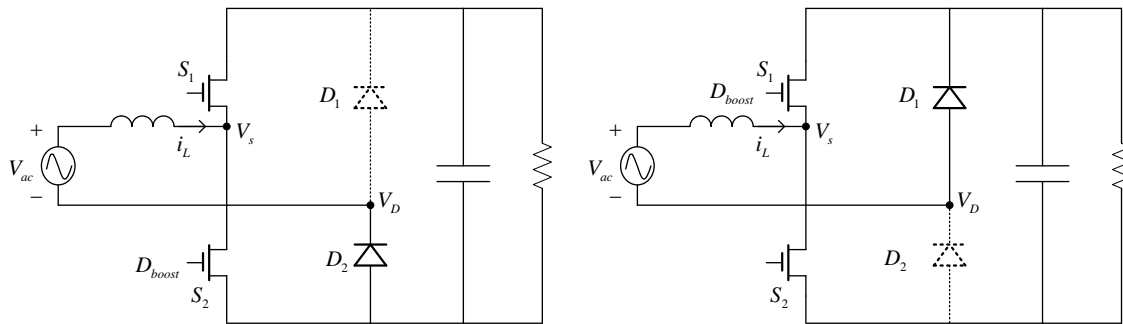


Fig.2 Operation principle of totem-pole bridgeless PFC (a) positive half cycle (b) negative half cycle.

Based on the operation principle, switch S1 and S2 work as freewheeling diodes in the boost circuit. Large reverse recovery charge (Q_{rr}) of existing silicon MOSFET makes the CCM operation of the totem-pole bridgeless PFC impractical, and reduces the total efficiency. Table 1 gives a comparison of CoolMOS and GaN HEMT. The low Q_{rr}, low switching loss GaN HEMT power device is the perfect device for this topology.

Table 1: Comparison of GaN HEMT with equivalent CoolMOS IPL60R199CP

	TPH3006LD/TPH3006LS	IPL60R199CP
ID	17A	16.4A
Ron	150 mΩ	180mΩ
Qg	6.2nC	32nC
Eoss(400V)	5uJ	6.1uJ
Qrr	54nC	5.5uC

One inherent issue in totem-pole bridgeless PFC is the operation mode transition at AC voltage zero-crossing. For instance, when the circuit operation mode changes from positive half line to negative half line at the zero-crossing, the duty ratio of switch S2 changes abruptly from almost 100% to 0%, and duty ratio of switch S1 changes from 0% to 100%. Due to the slow reverse-recovery of diodes (or body diode of MOSFET), the voltage V_D can not jump from ground to V_{DC} instantly, a current spike will be induced. To avoid the problem, a soft-start at every zero-crossing is implemented to gently reverse duty ratio. Since the proposed totem-pole bridgeless PFC is design to run in CCM, the larger inductance actually alleviates the current spike issue at zero-crossing. A soft-start time for a few switching cycles is enough to handle this problem.

Fig. 3 gives the overall control diagram for the totem-pole PFC with diode for line rectification. The voltage and current loop control are the same as conventional boost PFC converter. The feedback signals from the PFC are the V_{DC} , V_{AC-P} , V_{AC-N} and I_L . The input voltage polarity and Rms value are determined from V_{AC-P} and V_{AC-N} . The outer voltage loop output multiplied by $|V_{AC}|$ gives sinusoidal current reference. Current loop gives the proper duty-ratio for boost circuit. The polarity determined how PWM signal is distributed for switch S1 and S2. Soft-start duty ratio is used for a short-period after the zero-crossing.

The control of totem-pole PFC with MOSFET for synchronized line rectification is the same in Fig.3, with two additional driving PWM signals for the MOSFET during each half-cycle. Fig.4 shows the timing diagram for the driving signals of the active switch S_{D1} and S_{D2} . Switch S_{D2} will be turn-on after the soft-start at the beginning of positive half, while switch S_{D1} will be turn-on after the soft-start at the beginning of negative half. During the soft-start, when both MOSFETs are turn-off, they behave as diodes and the soft-start is the same as diode version of totem-pole bridgeless PFC.

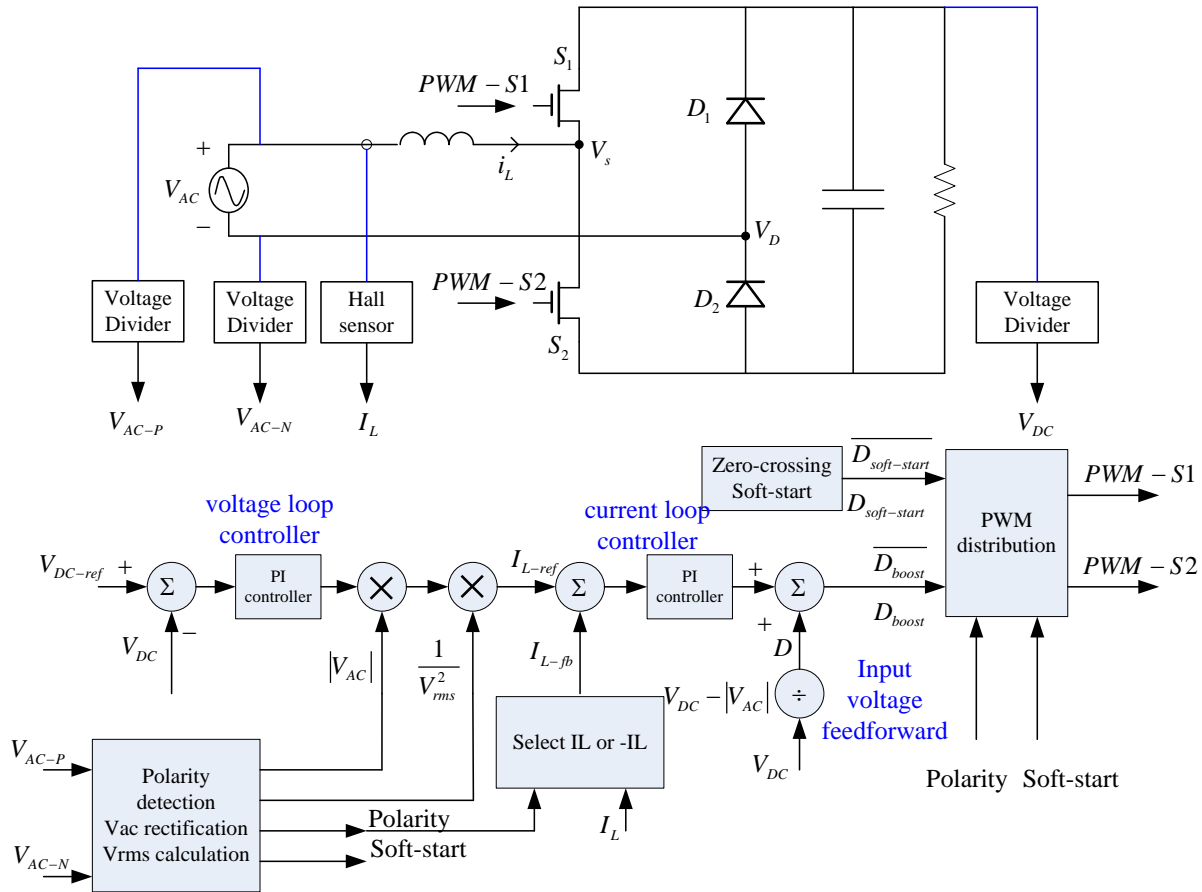


Fig.3 Over-all control diagram for the totem-pole bridgeless PFC in CCM

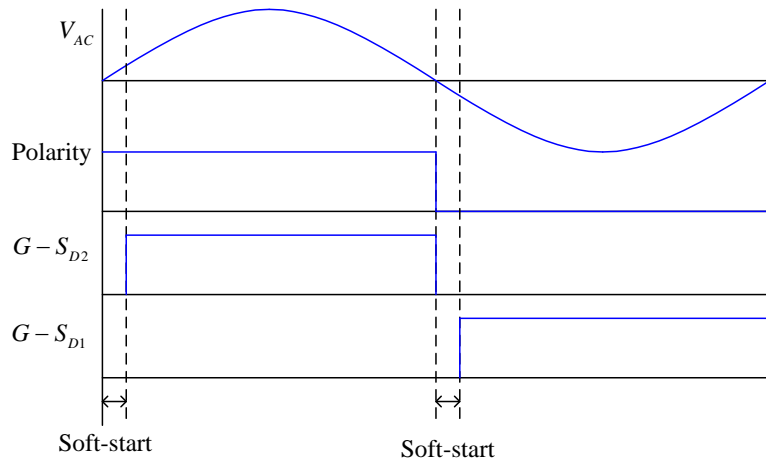


Fig.4 Gate signals timing for two active switches

To handle inrush current for bulk capacitor pre-charge during converter start-up, additional diodes are added in front of the inductor, so that inrush current will go through these two diodes instead of the body diode of HEMT. At the beginning of start-up, all active switches are turned off. Diode Dbp1, Dbp2 and the body diode of MOSFET Sd1, Sd2 formed a diode bridge to charge up the capacitors. GaN HEMT will then be

actively switched to ramp up the DC bus voltage is established.

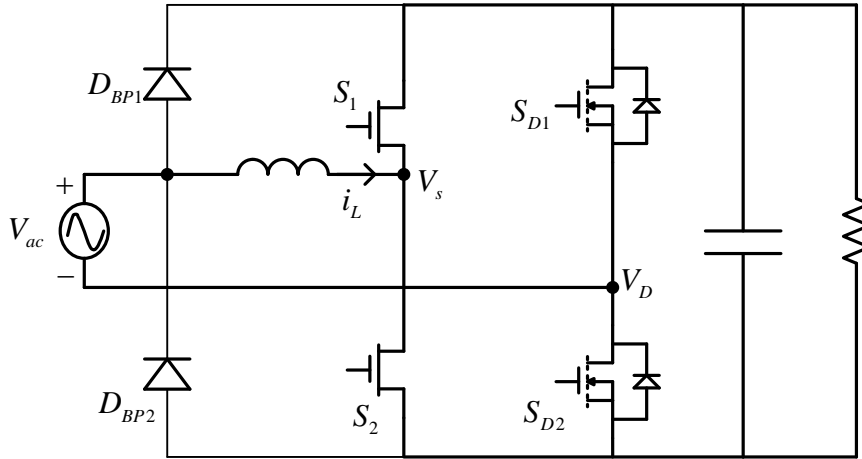


Fig.5 Two Diodes in front of inductor to bypass inrush current at converter start-up

IV. EXPERIMENTAL RESULTS

Both diode version and MOSFET version of totem-pole bridgeless PFC prototypes are built. The GaN HEMT half-bridge uses TPH3006LD and TPH3006LS developed by Transphorm Inc. GBJ2006 is used as the rectifiers in the diode version and two 100mΩ MOSFETs IPA60R099C6 are used as synchronized rectifiers in the MOSFET version. The inductors are built using MPP core 55439A2 from Magnetics with inductance of 1.3mH. The control algorithm is implemented on a low-cost, fixed-point 60MHz DSP controller TMS320F28027. The converter is running at a switching frequency of 50 KHz.

Fig. 6 gives pictures of both prototypes. High-side GaN HEMT TPH3006LD is on top, while the low-side GaN HEMT 3006LS is mounted on the bottom. Fig.7 shows the converter start-up, CH3 shows the DC bus voltage rapidly goes up at the beginning and then ramp up to 400V by control, while the inductor current is kept under 1A during the start-up process. Fig.8 and Fig.9 shows experimental waveform under 1KW full load. In Figure 8(a), voltage V_D is either 0V or 400V according to the operating mode. MOSFET S_{D2} is turned on during positive half cycle. Figure 8(b) shows the PFC functionality in an isolated oscilloscope. The power factor is 0.9998 according to power analyzer reading.

Fig.9 shows the transitions between two half cycles. In Fig.9(a), the AC line enters the negative half. Soft-start gradually increases voltage V_D from 0V to 400V. While in Fig.9(b), V_D decreases from 400V to 0V. Switch S_{D2} is turned on after the soft-start.

Efficiency is measured using precision power analyzer WT1800 from Yokogawa at 230Vac input, 400Vdc output. Fig.10 shows the efficiency measurement for diode version and active switch MOSFET version. Diode version efficiency peaks at 98.56% while MOSFET version peaks at 99.00%.

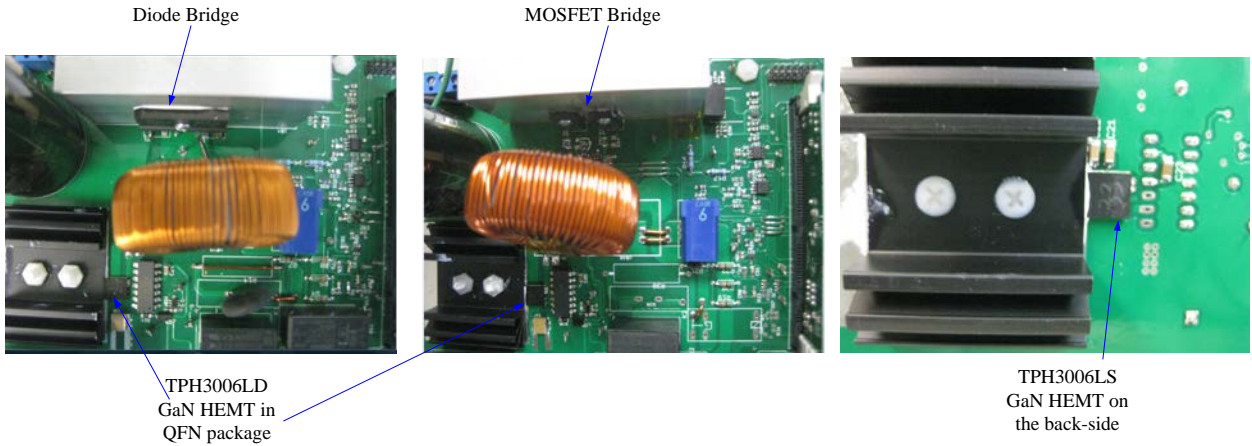


Fig.6 Pictures of the totem-pole bridgeless PFC prototypes

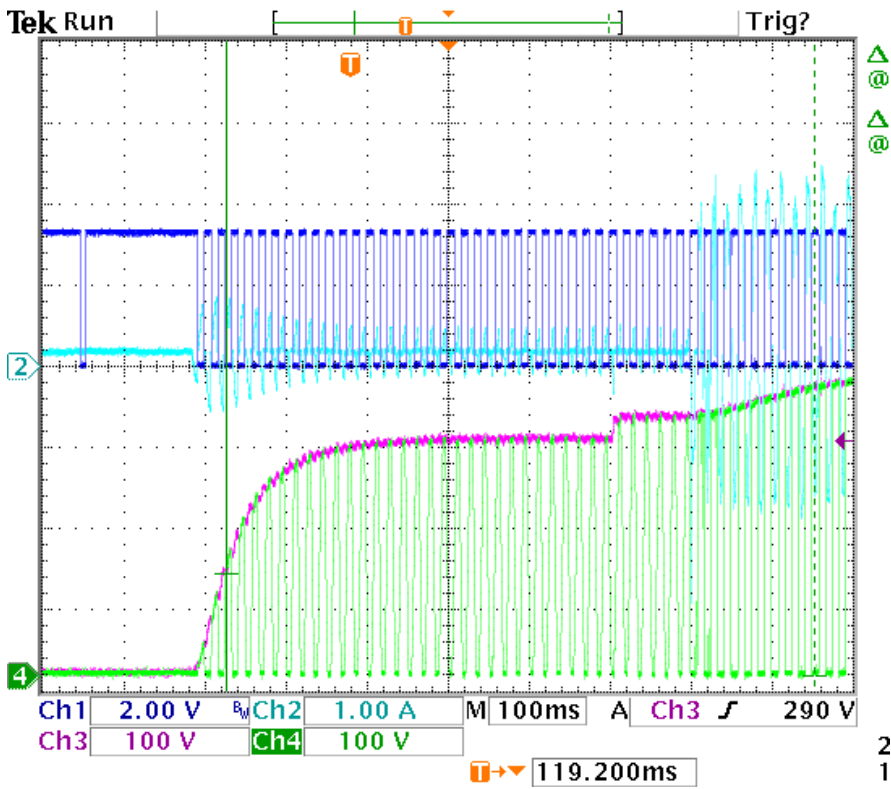
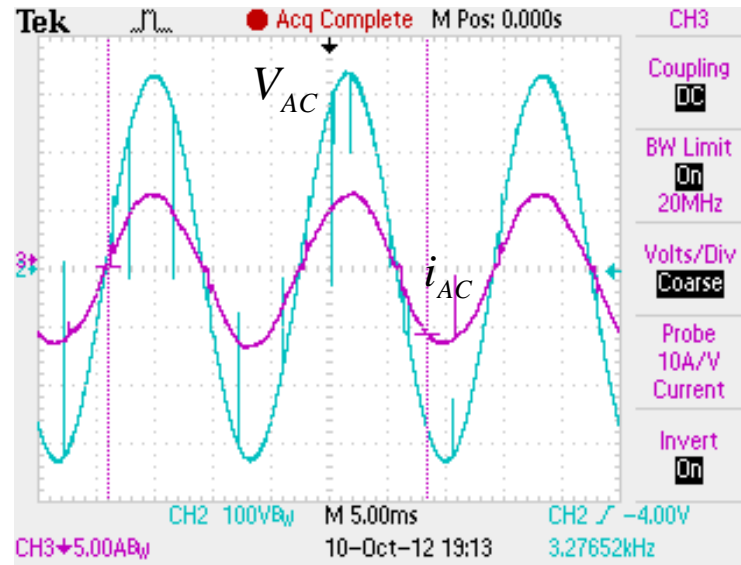
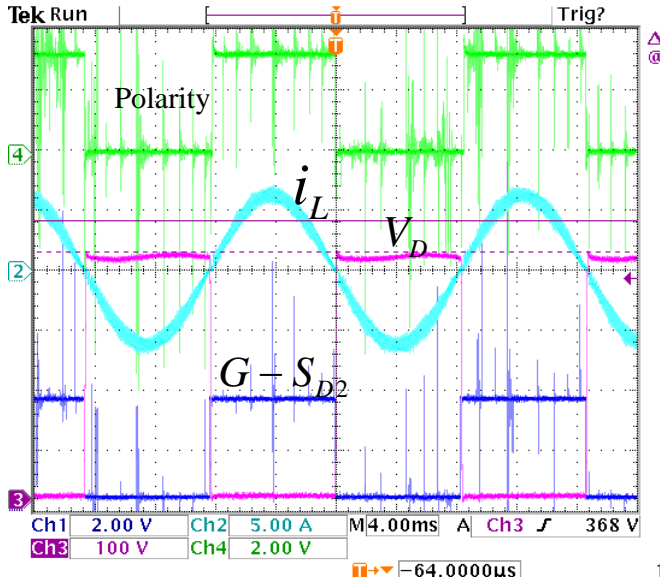


Fig.7 start-up of the totem-pole bridgeless PFC prototypes (CH1: AC Polarity, CH2: inductor current, CH3: Vo, CH4: Vd)



(a) CH1: PWM Gate signal for S_{D2} ; CH2: i_L waveform (5A/division); CH3: V_D waveform(100V/division); CH4: AC input polarity signal

(b) CH2: Input AC voltage(100V/division); CH3: input AC current (5A/division)

Fig.8 Waveform of the active switch version of the totem-pole bridgeless PFC at full load 1KW.

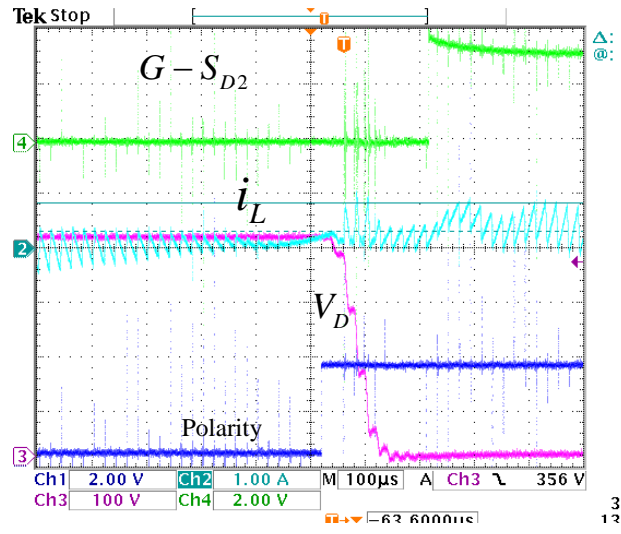
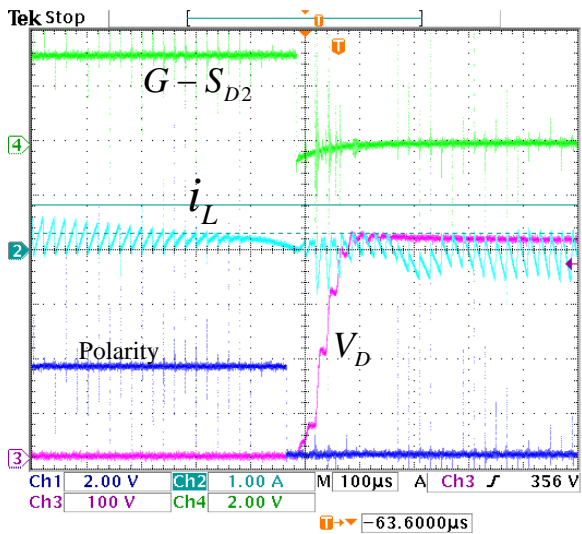


Fig. 9 Zero-crossing transitional waveform (a) from positive to negative half cycle (b) from negative to positive half cycle
CH1: AC input polarity; CH2: i_L waveform; CH3: V_D waveform; CH4: PWM gate for S_{D2}

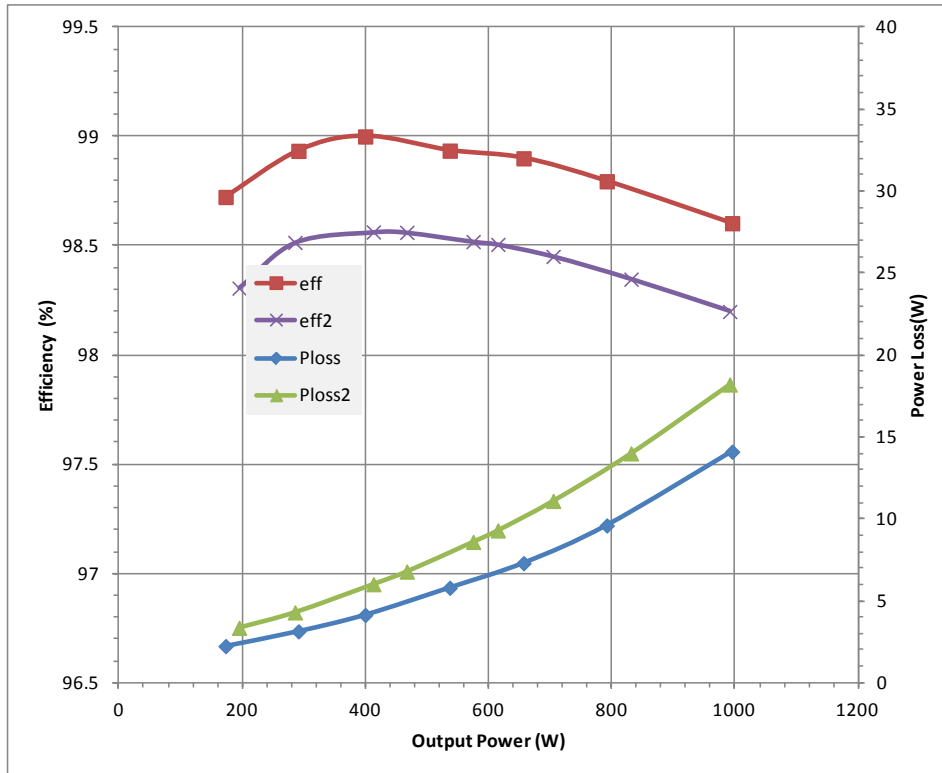


Fig.10 measured efficiency for both versions of totem-pole bridgeless PFC

(eff: MOSFET version efficiency; eff2: diode version efficiency; Ploss: MOSFET version power loss; Ploss2: diode version power loss)

V. CONCLUSION

High efficiency single phase totem-pole bridgeless PFC converters are presented in this paper based on GaN HEMT from Transphorm. The version with diodes as line rectifiers reaches 98.6% peak efficiency. Replacing the passive rectifiers by Silicon MOSFETs for synchronize line rectification, the peak efficiency is boosted to 99.0%. Depending on choice of control complexity, either circuit offers a high-efficiency, simple single phase PFC solution based on superior GaN HEMTs.

VI. REFERENCE

- [1] L. Huber, J. Yungtaek, and M. M. Jovanovic, "Performance Evaluation of Bridgless PFC Boost Rectifiers," *IEEE Trans. Power Electron.*, vol.23, no.3, pp.1381-1390, May 2008.
- [2] Q. Li, M.A.E. Andersen, and O.C. Thomsen, "Conduction Losses and Common Mode EMI analysis on bridgeless power factor correction," *International conference on Power Electronics and Drive Systems*, Nov. 2-5, 2009.
- [3] B. Su, J. Zhang and Z. Lu, "Totem-pole Boost Bridgeless PFC rectifier with simple zero-current detection and full-range ZVS operating at the boundary of DCM/CCM," *IEEE Trans. Power Electron.*, vol.26, no.2, Feb. 2011.

- [4] E. Firmansyah, S. Tomioka, S. Abe, M. Shoyama, and T. Ninomiya, "An interleaved totem-pole power factor correction converter," Research reports on information science and electrical engineering of Kyushu University, vol.15, no.1, Mar. 2010.
- [5] J. W. Kolar, F. Krismer, Y. Lobsiger, J. Muhlethaler, T. Nussbaumer and J. Minibock, "Extreme Efficiency Power Electronics," 7th international conference on integrated power electronics systems (CIPS), March, 2012.
- [6] Y.-F. Wu, D. Kebort, J. Guerrero, S. Yea, J. Honea, K. Shirabe and J. Kang "High-frequency GaN Diode-Free Motor Drive Inverter with Pure Sine-wave Output", PCIM, Nuremberg Germany, May 2012.
- [7] K. Shirabe, M. Swamy, Jun-Koo Kang, M. Hisatsune, Yifeng Wu, D. Kebort and J. Honea, "Advantages of high frequency PWM in AC motor drive applications," 2012 IEEE Energy Conversion Congress and Exposition (ECCE), 15-20 Sept. 2012.
- [8] Y.-F. Wu, R. Coffie, N. Fichtenbaum, Y. Dora, C.S. Suh, L. Shen, P. Parikh and U.K. Mishra, "Total GaN Solution to Electricity Power Conversion," the 69th IEEE Device Research Conference, Conference Digest, p217-218, June 20-22, 2011